DUAL BEAM ALONG-TRACK INTERFEROMETIC SAR TO MAP TOTAL OCEAN SURFACE CURRENT VECTORS WITH THE AIRBORNE WAVEMILL PROOF-OF-CONCEPT INSTRUMENT: IMPACT OF WIND-WAVES

A. Martin[1], C. Gommenginger[1], B. Chapron[2], J. Marquez[3], S. Doody[4], D. Cotton[5], C. Buck[6]

[1]National Oceanography Centre, Southampton, SO14 3ZH, UK
[2]IFREMER, Brest, France
[3]Starlab, Barcelona, Spain
[4]Airbus Defence & Space, UK
[5]Satoc, UK
[6]ESA/ESTEC, NL

ABSTRACT

Synoptic maps of total ocean surface currents from space are needed to improve the characterisation and parameterisations of oceanic sub-mesoscale dynamics and represent their impact on global ocean circulation, air-sea exchanges and the marine ecosystem. Wavemill is a satellite mission concept based on a dual beam along-track interferometric SAR principle. An airborne proof-of-concept campaign took place in the tidally-dominated Irish Sea in 2011. A comprehensive collection of airborne flights arranged in a star pattern permitted to sample various azimuthal directions. Here, it is shown that the impact of ocean waves on the measured ocean surface motion can be as large or even larger than the strong tidal current (0.7m/s). Using in situ validation measurements and airborne Wavemill data, the azimuth dependence and magnitude of this wind-wave velocity artefact is characterised.

Index Terms— SAR ATI, ocean surface current, wind, airborne experiment

1. INTRODUCTION

High-resolution satellite images of sea surface tempera- ture and ocean colour reveal a multitude of highly dy- namic small oceanic features that dominate the ocean variability at the mesoscale (10-100km) and sub-mesoscale (1-10km). Features such as eddies, fronts and filaments are ubiquitous and have been associated with energetic upper ocean dynamics and mixing processes. There is growing scientific evidence that these small oceanic scales play a major role for horizontal and vertical mixing, large-scale oceanic transport and ocean biology. For example, 50% of the vertical transport of ocean biogeochemical properties is thought to take place at scales smaller than 100km [1], while ageostrophic secondary circulation associated with eddies produce very large upwelling velocities of the order of 10 m/day [2]. Improved characterisation of these small scale features is needed to develop improved parameterizations to represent these sub-mesoscale processes in models used for long-term climate predictions. Thus, with the response of the ocean biosphere to climate change remaining one of the greatest uncertainties in climate projections, there is a strong demand for synoptic observations of the ocean surface total current fields at these small scales.

Today, none of the available satellite techniques are able to provide direct measurements of these quantities with sufficient accuracy and resolution. Sequences of satellite sea surface temperature or ocean colour images can provide estimates of advection by tracking features from image to image using the Maximum Cross-Correlation method [3] but the method is affected by cloud and relies on the presence of strong trackable features in successive images. Satellite altimeters give all-weather day-and-night estimates of currents globally, based on differences in sea surface height from which the geostrophic component of the currents can be estimated. But the altimeters narrow swaths, large track-to-track separation and reliance on coarse geoid data mean that altimeters cannot resolve features below 70-100 km scales. This well-known limitation of nadir altimetry is the prime motivation for the NASA/CNES Surface Water and Ocean Topography (SWOT) mission, which will rely on cross-track interferometry to deliver two-dimensional maps of sea surface height at 1km resolution [4].

Direct estimates of total surface currents can be obtained with satellite Synthetic Aperture Radar (SAR) by measuring the shift of the Doppler spectrum centroid in a method pioneered by [5]. More recently, significant advances in spaceborne measurements of currents were made possible thanks to along-track interferometric SAR experiments onboard TerraSAR-X [6, 7]. However, even though these techniques do deliver total currents with useful spatial resolution and accuracy, they only provide one component of the current

in the direction of the instrument line-of-sight.

The Wavemill instrument concept was originally conceived by [8]. The present configuration is a Ku-band dual beam SAR ATI. The dual beams have 45^o squint at the surface which permits to look the sea surface with two direction then providing a current vector. The incidence angle at mid-swath is of 30^o.

A Wavemill airborne proof-of-concept experiment took place on 25 and 26 October 2011 nights with flights over various sites in the Irish Sea, Liverpool Bay and Anglesey areas off the west coast of the United Kingdom (See Fig. 1).

Here, airborne Wavemill data are analysed that were acquired on the night of the 25th to 26th of October 2011 above the well-instrumented Mersey Bar Light station. Data were acquired during a maximum ebbing tidal flow (≈0.7m/s). After a brief presentation of the available airborne data and the geophysical conditions during the flights, the theoretical basis to estimate radial surface velocity is described, together with an introduction to the problem of wind-wave surface velocity artefacts in SAR-derived surface velocity estimates. An estimation of the wind-wave surface velocity artefact observed in the Wavemill airborne data will be presented in section 4.

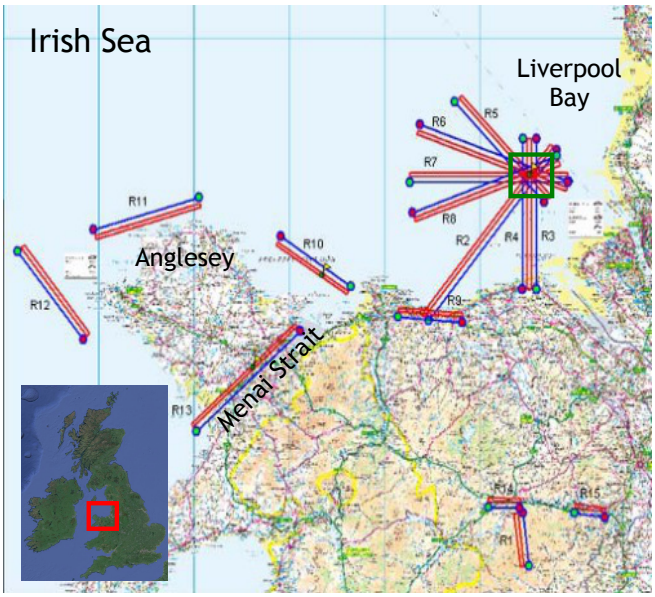

Fig. 1. Location of Wavemill airborne proof-of-concept flights over the Irish Sea/Liverpool Bay/Anglesey area off the west coast of the UK. The various Wavemill runs are denoted as R2, R3, ... The dark green square indicates the data in the star pattern centred over the Mersey Bar Light which are considered in this paper.

2. EXPERIMENTAL DATA

2.1. Wavemill airborne proof-of-concept data

Data was acquired with the X-band Wavemill airborne demonstrator instrument developed by Airbus Defence and Space, deployed onboard a Douglas DC-3 aircraft. Acquisitions were carried out in single-pass mode using two pairs of antennas: two looking fore and two looking aft of the aircraft. The mean squint angle at the surface for each antenna is $\pm 45^o$. One antenna operated in transmit/receive mode (monostatic channel), while the second operated in receive mode only (bistatic channel). The campaign resulted in the flight paths shown in Figure 1. The focus here is on the seven runs arranged in a star pattern above the Mersey Bar Light marked with a dark green square on the figure.

The two pairs of antennas are mounted on a gimbal which corrects for the aircraft roll and yaw (but not the pitch). The effective baseline (B_{eff}) between the two antennas of each pair is 25cm. The mean aircraft velocity (V) is 80m/s leading to a time lag (τ) between the two antennas of 3ms which is short enough to ensure signal coherence. The spatial resolution of the high-resolution products is better than 5m (along and across track). The incidence angle is between 26.3^o (near range) and 44.0^o (far range).

2.2. Geophysical conditions

The geophysical conditions described here are for Liverpool Bay on the 26th of October 2011 between 00h and 01h30 UTC i.e. at the time of the airborne flights. These conditions were estimated thanks to various in situ observations (e.g. ADCP, HF radar, wave buoy) and atmospheric wind model output from the UK MetOffice. To summarise, the tidal current was very stable during the runs with a value around 0.7m/s flowing in a 270^o direction (westward). The wind is from the South (190^o) and about 5m/s. There is in addition a weak swell system from the North-West ($H_s = 0.5$m, $\lambda = 70$m) leading to a mixed sea. Water depth in the vicinity of Mersey Bar Light is fairly constant and around 20 metres.

3. THEORETICAL BASIS

3.1. Retrieving radial surface velocity

The pixel-by-pixel phase difference between the two complex SAR images is called the interferogram ($\Delta\phi$) and is simply the product of the mean Doppler frequency ($\overline{\omega}$) and the time lag (τ) between the two SAR images [9, 10]. The time lag is related to the separation between the two antennas in the along-track direction and the platform velocity. The interferogram gives a measure of the velocity in the line-of-sight. The radial surface velocity is the projection of the line-of-sight velocity on the surface (function of mean Doppler frequency),

i.e. using the Wavemill parameters:

$$U_{surf} = \Delta\phi \frac{\lambda_e V}{2\pi B_{eff} \sin\theta}; \quad (1)$$

$$\approx \frac{0.7\Delta\phi}{\sin\theta}; \quad (2)$$

with λ_e the radar wavelength, $\Delta\phi$ the interferogram, V the aircraft velocity, B_{eff} the effective baseline and θ the incidence angle.

3.2. Wind-wave Surface Velocity artefacts

The surface velocity measured by SAR sensors has been shown to be highly correlated with the wind speed (about 30% of the wind component, [5]). This observed velocity artefact has been attributed to the correlation between the wave-induced tilt modulation of the NRCS (Normal Radar Cross Section) and the wave-induced orbital velocity [11, 5]. This correlation is well illustrated in Figure 6 in [5].

4. OBSERVED WIND-WAVE SURFACE VELOCITY ARTEFACT IN AIRBORNE WAVEMILL MEASUREMENTS

The radial surface velocity (U_{surf}) for each pair of antennas was derived from the interferogram ($\Delta\phi$) according to (1). To examine the wind-wave surface velocity artefact present in the Wavemill measurements, the relevant component of the surface current measured by the ADCP has been removed from the radial surface velocity. Thus, what remains should correspond only to the wave-induced artefact current . This is shown in Fig. 2 for two incidence angles corresponding to the near and far range. Both curves have a quasi sinusoidal shape with extrema in the upwind/downwind direction (close to $180^o/0^o$). The artefact velocity is minimal in the crosswind direction. The amplitude is stronger at near range (upwind at 1.5m/s for 26^o incidence) than at far range (upwind at 1m/s for 44^o incidence). In absolute value, the upwind artefact velocity is about 0.5m/s higher than the downwind, whatever the incidence angle. The magnitude and azimuth dependence of the observed artefact velocity is in excellent agreement with the estimates obtained from satellite ENVISAT/ASAR measurements in C-band for a wind speed of 5m/s [12].

The wind-waves artefact velocity calculated with a simple theoretical model [5] using the Mersey Bar Light in situ wave spectrum and an empirical NRCS geophysical model function (interpolated from CMOD and NSCAT to X-band) also show very good agreement with the Wavemill results in terms of azimuth dependence and the decrease in magnitude with incidence angle (not shown). However, this simple model predicts higher absolute values of the artefact velocity in the downwind direction than upwind, which is opposite of the observations (both from satellite [12] and the airborne Wavemill Proof-of-Concept data). More advanced models seem better able to correctly reproduce this upwind/downwind asymmetry [13, 14].

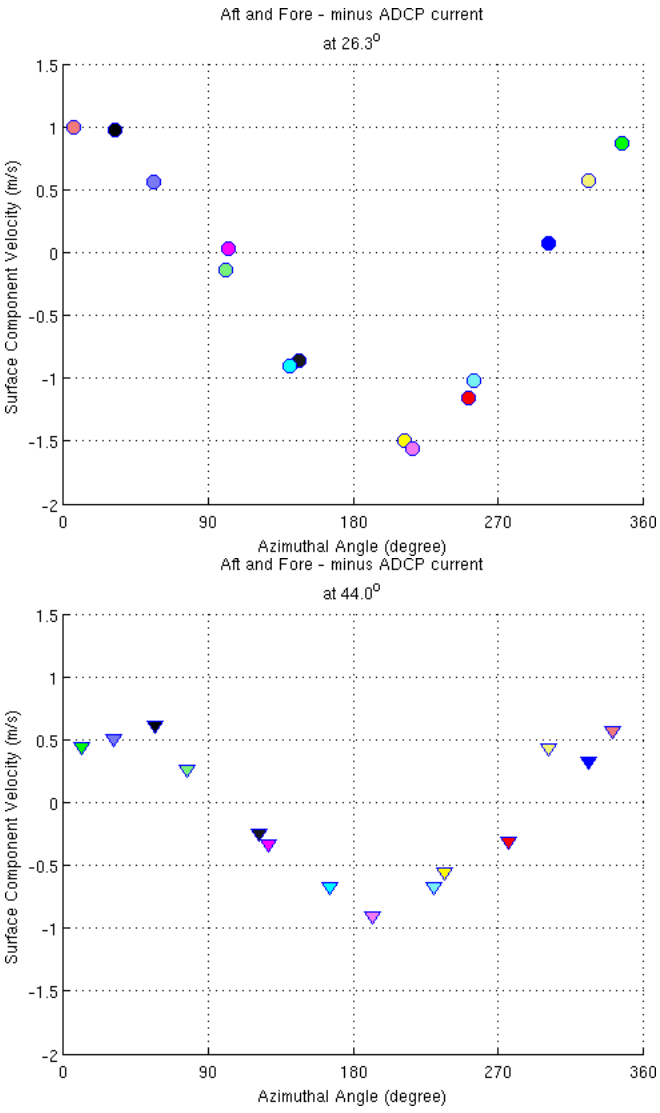

Fig. 2. Wind-wave artefact velocity observed in the Wavemill airborne Proof-of-Concept data computed as the measured surface velocity minus the sea surface current measured by the ADCP. Velocity is in m/s shown as a function of azimuth direction with respect to North(0 deg). (top) Results for near range at 26.3^o incidence. (bottom) Results for far range at 44.0^o incidence. Colours represent the different runs. Darker colours correspond to the aft antenna pair and pastel colour to the fore antenna pair.

5. CONCLUSIONS & PERSPECTIVES

The Wavemill airborne Proof-of-Concept experiment confirms the very strong impact of wind-waves on the surface

velocity Doppler measurements. For the geophysical conditions encountered during the Irish Sea experiment (wind speed of 5m/s, tidal current of 0.7 m/s), the wind-wave artefact velocity in the upwind direction reaches 1.5m/s at 26^o incidence and 1m/s at 44^o incidence i.e. up to 30% of the wind speed. The airborne star pattern offered the perfect means to explore the dependence with azimuth direction and emphasised in particular the strong upwind/downwind asymmetry in magnitude, with the upwind value about 0.5m/s higher (in absolute value) than the value downwind, whatever the incidence angle (in the range 26–44^o). These airborne results are in excellent agreement with the estimates derived from satellite ENVISAT/ASAR data[12].

The Wavemill Proof-of-Concept data were acquired for very particular geophysical conditions (mixed sea with a low-amplitude swell crossing a fetch limited wind-sea, wind of 5 m/s). More airborne experiments are needed in other geophysical conditions to improve our understanding and our ability to model and remove these important wind-wave artefact effects. A good correction of the wind-wave artefact velocity is absolutely necessary in order to retrieve sea surface current vectors with sufficient accuracy.

Finally, the Wavemill airborne demonstrator data were acquired in VV polarisation, but both the satellite data [12] and models e.g. [14] show differences in the wind-wave artefact velocity observed at VV and HH polarisation. As VV and HH have the same response to sea surface current, simultaneous acquisition in dual-polarisation could offer a solution to estimate and remove wind-wave artefact effects. In this perspective, it will be necessary to improve too our understanding of wave artefact effects in HH polarisation, which will need further technological and modelling developments.

6. REFERENCES

[1] Guillaume Lapeyre and Patrice Klein, "Impact of the small-scale elongated filaments on the oceanic vertical pump," *Journal of Marine Research*, vol. 64, no. 6, pp. 835–851, 2006.

[2] Adrian P. Martin and Kelvin J. Richards, "Mechanisms for vertical nutrient transport within a north atlantic mesoscale eddy," *Deep Sea Research Part II: Topical Studies in Oceanography*, vol. 48, no. 4–5, pp. 757 – 773, 2001, The Biological Oceanography of the north-east Atlantic-the {PRIME} study.

[3] W. J. Emery, A. C. Thomas, M. J. Collins, W. R. Crawford, and D. L. Mackas, "An objective method for computing advective surface velocities from sequential infrared satellite images," *Journal of Geophysical Research: Oceans*, vol. 91, no. C11, pp. 12865–12878, 1986.

[4] L.-L. Fu, D.B. Chelton, P.-Y. Le Traon, and R. Morrow, "Eddy dynamics from satellite altimetry," *Oceanography*, pp. 14–25, 2010.

[5] Bertrand Chapron, Fabrice Collard, and Fabrice Ardhuin, "Direct measurements of ocean surface velocity from space: Interpretation and validation," *Journal of Geophysical Research: Oceans*, vol. 110, no. C7, 2005.

[6] R. Romeiser, S. Suchandt, H. Runge, U. Steinbrecher, and S. Grünler, "First analysis of terrasar-x along-track insar-derived current fields," *Geoscience and Remote Sensing, IEEE Transactions on*, vol. 48, no. 2, pp. 820–829, 2010.

[7] R. Romeiser, H. Runge, S. Suchandt, R. Kahle, C. Rossi, and P.S. Bell, "Quality assessment of surface current fields from terrasar-x and tandem-x along-track interferometry and doppler centroid analysis," 2013.

[8] C. Buck, "An extension to the wide swath ocean altimeter concept," in *Geoscience and Remote Sensing Symposium, 2005. IGARSS '05. Proceedings. 2005 IEEE International*, July 2005, vol. 8, pp. 5436–5439.

[9] D. R. Thompson and J. R. Jensen, "Synthetic aperture radar interferometry applied to ship-generated internal waves in the 1989 loch linnhe experiment," *Journal of Geophysical Research: Oceans*, vol. 98, no. C6, pp. 10259–10269, 1993.

[10] Hans C. Graber, Donald R. Thompson, and Richard E. Carande, "Ocean surface features and currents measured with synthetic aperture radar interferometry and hf radar," *Journal of Geophysical Research: Oceans*, vol. 101, no. C11, pp. 25813–25832, 1996.

[11] D. R. Thompson, B. L. Gotwols, and W. C. Keller, "A comparison of ku-band doppler measurements at 20° incidence with predictions from a time-dependent scattering model," *Journal of Geophysical Research: Oceans*, vol. 96, no. C3, pp. 4947–4955, 1991.

[12] A.A. Mouche, F. Collard, B. Chapron, K. Dagestad, G. Guitton, J.A. Johannessen, V. Kerbaol, and M.W. Hansen, "On the use of doppler shift for sea surface wind retrieval from sar," *Geoscience and Remote Sensing, IEEE Transactions on*, vol. 50, no. 7, pp. 2901–2909, 2012.

[13] A. A. Mouche, B. Chapron, N. Reul, and F. Collard, "Predicted doppler shifts induced by ocean surface wave displacements using asymptotic electromagnetic wave scattering theories," *Waves in Random and Complex Media*, vol. 18, no. 1, pp. 185–196, 2008.

[14] M.W. Hansen, V. Kudryavtsev, B. Chapron, J.A. Johannessen, F. Collard, K.-F. Dagestad, and A.A. Mouche, "Simulation of radar backscatter and doppler shifts of wave–current interaction in the presence of strong tidal current," *Remote Sensing of Environment*, vol. 120, no. 0, pp. 113 – 122, 2012, The Sentinel Missions - New Opportunities for Science.